Facile Synthesis of Macroporous Cross-Linked Methacrylate Gels by Atom Transfer Radical Polymerization

Kazuyoshi Kanamori,* Joji Hasegawa, Kazuki Nakanishi, and Teiichi Hanada

Department of Chemistry, Graduate School of Science, Kyoto University, Kitashirakawa, Sakyo-ku, Kyoto 606-8502, Japan

Received March 13, 2008; Revised Manuscript Received July 22, 2008

ABSTRACT: Macroporous cross-linked organic polymer monoliths with well-defined bicontinuous structure have been synthesized from 1,3-glycerol dimethacrylate (GDMA) in a solvent utilizing atom transfer radical polymerization (ATRP). With the addition of an adequate polymeric agent, poly(ethylene oxide) (PEO), spinodal decomposition was induced in the course of polymerization of GDMA. A homogeneous gelation by ATRP solidified the temporal biphasic morphology of spinodal decomposition, resulting in well-defined macroporous gels after drying. Macroporous dried gels obtained in this way comprise interconnected skeletons and macropores, which is characteristic for spinodal decomposition. Macropore size and volume were controlled simply by altering the starting composition. The mechanism of spinodal decomposition is deduced that the separation takes place between polymerizing GDMA and PEO, but FTIR and thermal analyses suggested the amount of PEO that is distributed in GDMA-rich phase cannot be neglected. Free radical polymerization, which is generally utilized for synthesis of porous polymeric gels, usually leads to heterogeneous cross-linking forming local microgels and hinders the occurrence of spinodal decomposition in a cross-linking system over extended length scales. On the other hand, living polymerization allowed homogeneous cross-linking; hence, isotropic spinodal decomposition was induced in the copresence of PEO. The facile synthesis method presented here will lead to more precise control of pore properties of cross-linked organic polymer gels.

1. Introduction

Porous materials have a broadened range of applications such as separation media, catalyst supports, adsorbents, and filters. In addition to the sufficient surface area which allows molecular-level contact of the guest substances with the material, efficient liquid transport through the porous body becomes crucial in exploring better total performance in the above applications. Bicontinuous macroporous structure, which is developed by spinodal decomposition and contains three-dimensionally co-continuous solid skeletons and macropores in the micrometer range, has been proved to be the most promising candidate for these purposes because it allows a fast liquid transport through the continuous macropores.[1−3] We, for the first time, reported the preparation of sol−gel silica with well-defined bicontinuous structure by spinodal decomposition using a coexisting polymer such as sodium polystyrenesulfonate, poly(acrylic acid), and poly(ethylene oxide) or using a polar solvent such as formamide or methanol.[4,5] In these cases, the silicate species become less soluble in the solvent with the progresses of polymerization because of the thermodynamic destabilization induced by increased free energy of mixing of entropic and/or enthalpic origins. This induces phase separation directed by the "chemical cooling" process in which the progress of polymerization, instead of decreased temperature as in the "physical cooling", brings an originally homogeneous mixture into that with multiple phases. In the process of spinodal decomposition, a small concentration fluctuation arises in the original single phase medium and eventually forms double phase with a bicontinuous configuration. One phase containing a polymerizing component such as silicate will subsequently solidify the temporal morphology to result in bicontinuous macroporous structure after drying (and heat treatment). This kind of sol−gel silica or siloxane-based organic−inorganic hybrid gels with bicontinuous structure, which are often referred to porous silica monoliths, have already been used as highly efficient separation media for high-performance liquid chromatography (HPLC) due to the fast liquid transport.[1] Especially, porous gels simultaneously having macropores (∼1 μm) and mesopores (∼10 nm) affords the large surface area in addition to the fast liquid transport, which effectively enhances the interaction between analytes and the stationary phase.

However, since silica is chemically unstable and dissolves under basic aqueous conditions, it is desired to tailor monolithic HPLC beds composed of cross-linked polymer gels, which are stable under such conditions, with comparative separation efficiency as silica monoliths. In monolithic cross-linked porous gels consisting of cross-linked organic polymer (often referred to polymer monoliths), a so-called cauliflower-like morphology is generally obtained via conventional radical polymerization with utilizing typically low molecular weight solvent, polymeric additives, or their mixtures as "porogens".[6−9] In such monoliths, precise control over macropore size and volume is rather difficult. Above all, micropores and mesopores are not well-regulated due to the poorly controllable polymerization reactions by conventional free radial mechanisms. Polymer monoliths therefore generally show lower separation efficiency of small molecules compared to silica monoliths. To date, very few have been reported on the synthesis of polymer monoliths with well-defined bicontinuous macroporous morphology based on spinodal decomposition, though such monoliths are expected to improve the separation. Tsujioka et al.[10] reported a successful preparation of macroporous epoxy resins with well-defined macroporous structure via polycondensation reaction under the presence of a polymeric agent, poly(ethylene oxide). As they pointed out, however, the majority of polymer monoliths so far have been prepared via radical polymerization of vinyl monomers, and therefore the related techniques including surface modifications have also been developed on vinyl polymers. For these reasons, well-defined macroporous polymer gels derived from vinyl monomers are highly desired.

While in the effort of better controlling porous structures of polymer monoliths, the groups of Svec[11,12] and Buchmeiser[13,14]

* Corresponding author: Fax +81-75-753-7673; e-mail kanamori@kuchem.kyoto-u.ac.jp.

10.1021/ma800563p CCC: $40.75
Published on Web 09/04/2008

Table 1. Starting Compositions and Sample Notations[a]

	GDMA/g	DMF/mL	PEO/g
D4-P0.15	3.23	4	0.150
D4-P0.20	3.23	4	0.200
D4-P0.25	3.23	4	0.250
D5-P0	3.23	5	0
D5-P0.20	3.23	5	0.200
D5-P0.25	3.23	5	0.250
D5-P0.30	3.23	5	0.300
D6-P0.25	3.23	6	0.250
D6-P0.30	3.23	6	0.300
D6-P0.35	3.23	6	0.350

[a] The amounts of other compounds are fixed as follows: HMTETA 0.020 mL, Cu(I)Br 0.010 g, and MBPA 0.010 mL. Hence, [GDMA]/[MBPA]/[CuBr]/[HMTETA] molar ratio is 100/0.45/0.49/0.52.

applied nitroxide-mediated living radical polymerization (NMP) and ring-opening metathesis polymerization (ROMP), respectively. Both groups found better and broader controllability of porosity and microstructure, which resulted from the more homogeneous cross-linking reactions by living polymerizations. Also, the monoliths were able to be further functionalized or derivatized using living radical species still existing on the surface even after gelation.

In this current research, we have recently reported the preparation of well-defined bicontinuous poly(divinylbenzene) (PDVB) gels prepared from nitroxide-mediated living radical polymerization (NMP).[15] By incorporating a polymeric agent poly(dimethylsiloxane) (PDMS), which becomes incompatible during the polymerization of DVB, the spinodal-type phase separation was induced, and it was demonstrated that pore size and pore volume are independently controllable. However, NMP restricts the usage of monomers within styrenes and also requires relatively high temperature (~125 °C). To broaden the selection of monomers and reduce the reaction temperature to make the process easier, we in the present study extend this idea to another typical living radical polymerization system, atom transfer radical polymerization (ATRP),[16,17] to prepare cross-linked macroporous polymer gels using 1,3-glycerol dimethacrylate (GDMA) as a monomer. The hydrophilic property of the surface of GDMA-derived gels due to the inherent hydroxyl group is recently finding applications to the solid-phase peptide synthesis and separation media in HPLC, etc.[18−20] In this study, poly(ethylene oxide) (PEO, M_v = 100 000) has been employed as a polymeric agent to induce phase separation because of its good solubility in a starting solution and appropriate phase separation tendency against polymerizing GDMA to obtain macroporous gels.

2. Experimental Section

All chemicals used in this study were used as received. The typical starting compositions are provided in Table 1. Given amounts of 1,3-glycerol dimethacrylate (GDMA, Wako Pure Chemical Ind. Ltd., Japan), poly(ethylene oxide) (PEO, M_v = 100 000, Aldrich), 1,1,4,7,10,10-hexamethyltriethylene tetramine (HMTETA, Aldrich), and copper(I) bromide (Cu(I)Br, Aldrich) were dissolved in the solvent *N*,*N*-dimethylformamide (DMF, Hayashi Pure Chemical Ind. Ltd., Japan). After 3 min ultrasonic degassing and 15 min purging with nitrogen, the initiator methyl α-bromophenylacetate (MBPA, Aldrich) was added to trigger the polymerization reaction, which was then transferred into a glass ampule and allowed to gel at 70 °C in an oil bath. The typical gelation time was ~2.5 h. After reacting for 48 h, the resultant gel was soaked in an excess amount of water/ethanol (1/1 in volume) solution for 24 h at 60 °C to remove the unreacted monomers and PEO, etc., followed by a solvent-exchange with tetrahydrofuran (THF, Hayashi Pure Chemical Ind. Ltd., Japan) for 24 h at 60 °C. Drying was then conducted by evaporation in a convection oven at 60 °C for more than 48 h.

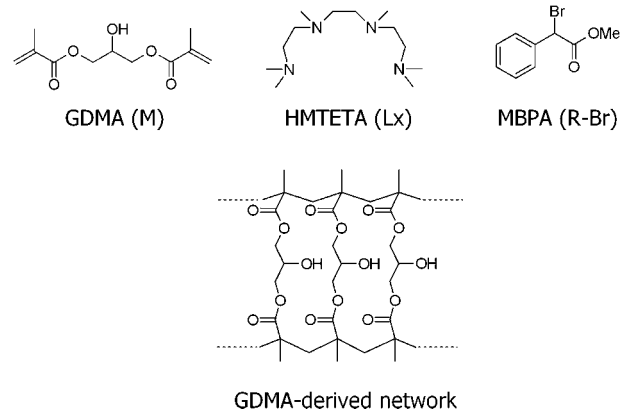

Figure 1. Molecular structures of the chemical agents used in this study and simplified network structure derived from GDMA.

Swelling experiments were performed to assess the good solvent for the GDMA-derived network. Gels prepared with the composition D5-P0 were solvent-exchanged in a variety of amidic and alcoholic solvents: 1-octanol (OctOH, δ_s = 10.3), 2-methyl-2-propanol (*tert*-BuOH, δ_s = 10.6), *N*,*N*-dimethylacetamide (DMAc, δ_s = 10.8), 1-butanol (BuOH, δ_s = 11.4), 2-propanol (*sec*-PrOH, δ_s = 11.5), 1-propanol (PrOH, δ_s = 11.9), *N*,*N*-dimethylformamide (DMF, δ_s = 12.0), benzyl alcohol (BzOH, δ_s = 12.1), ethanol (EtOH, δ_s = 12.7), methanol (MeOH, δ_s = 14.5), *N*-methylacetamide (NMAc, δ_s = 14.6), *N*-methylformamide (NMF, δ_s = 16.1), and formamide (FA, δ_s = 19.2). Here δ_s denotes the solubility parameter in $cal^{1/2}$ $cm^{-3/2}$. The swelling coefficient Q was obtained by $Q = (W_{swell} - W_{dry})/dW_{dry}$, where W_{swell} and W_{dry} correspond to the weight of swollen and dried gels, respectively, and d shows the density of the solvent. The gel fraction (the percentage of monomer molecules that have been incorporated in a solid network) was obtained by weighing washed and dried samples that were taken out of the oil bath in defined time intervals after gelation. Reduced time t_R/t_G, where t_R and t_G give the reaction time and gelation time, respectively, is used to determine the reaction time dependency of gel fraction.

The microstructure of the resultant dried gel was observed under SEM (JSM-6060S, JEOL, Japan). To assess the pore diameter D_p and volume V_p, mercury intrusion porosimetry (Poremaster 60-GT, Quantachrome Corp.) was employed. A cylindrical pore was assumed to transform the intrusion pressure into the pore diameter using the Washburn equation. Skeletal density, d_s, was measured by using He pycnometry (AccuPyc 1330, Micromeritics), and porosity ρ was obtained from the equation ρ (%) = 100 × $V_t/(V_t + 1/d_s)$, where V_t denotes the total pore volume obtained by mercury porosimetry. Molecular structure was investigated by FTIR (FTIR-8300, Shimadzu, Japan) with an attenuated total reflection (ATR) apparatus. For each measurement, a hundred scans were averaged at a resolution of 4 cm^{-1}. Thermal analyses of the obtained gels were conducted by TG-DTA (Thermo plus TG 8120, Rigaku, Japan) at a rate of 10 °C min^{-1} while continuously supplying air at a rate of 100 mL min^{-1}.

3. Results and Discussion

3.1. Gelation of the GDMA−DMF System via ATRP. Figure 1 depicts the structure of chemical agents used in this study and the GDMA-derived network that should be obtained in the ATRP process shown in Scheme 1 (after ref 16). The network structure is obviously oversimplified; it should be formed with a random distribution of cross-linking points and disordered molecular configurations, resulting in an amorphous network. In the present system with a ligand HMTETA in the solvent DMF, ATRP reactions are allowed to occur in a homogeneous medium. Using a sample prepared without PEO (D5-P0), we first investigated the swelling behavior to know the good solvent for the GDMA-derived network because a poor

Scheme 1. Reaction Scheme for ATRP (See Figure 1 for Symbols)

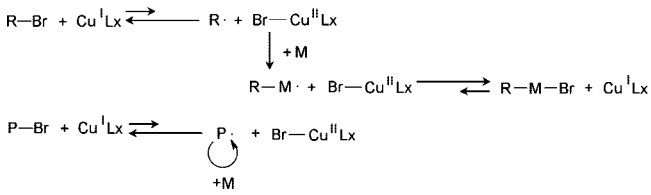

solvent may induce heterogeneity with submicron or even micron scale that hampers the occurrence of spinodal decomposition as discussed later. Figure 2a shows the result of the swelling test with a sample D5-P0. It is known that the extent of swelling is largely influenced by the interaction parameter χ between polymer and solvent, which is proportional to the difference between solubility parameters of them. However, it can be seen that amides tend to swell more than alcohols irrespective of the values of solubility parameter probably due to the more effective hydrogen bonding. With disregard to this exceptional swelling by amides, the most swelling solvents are BzOH and DMF, and the solubility parameter of the gel can be deduced to be ca. 12 cal$^{1/2}$ cm$^{-3/2}$.

In addition, to assess the sufficient reaction time, the time dependence of gel fractions was also investigated. Figure 2b demonstrates the gel fraction vs reaction time reduced with gelation time. Since the reaction terminates within $t_R/t_G < 10$ and typical t_G was 2.5 h (somewhat varied depending on the starting composition), the samples should be reacted for >25 h to complete at 70 °C.

3.2. Morphologies and Properties of GDMA-Derived Macroporous Gels. Gels prepared without PEO such as D5-P0 did not show any porosity after evaporative drying. By incorporating PEO with an appropriate molecular weight (M_v = 100 000 in the present system), dried gels with bicontinuous macroporous morphologies, in which both continuous gel skeletons and macropores are three-dimensionally connected, are obtained in a broadened compositional range, as depicted in Figure 3. For lower molecular weight PEO with M_n = 10 000, we could not obtain bicontinuous structure because phase separation tendency was too small. Conversely, for higher molecular weight PEO with M_v = 1 000 000, it was difficult to control pore properties because phase separation tendency was too high. For these reasons, we investigated the phase separation behavior using PEO with M_v = 100 000. In Figure 3, it can be interpreted that increasing PEO while fixing GDMA/DMF and

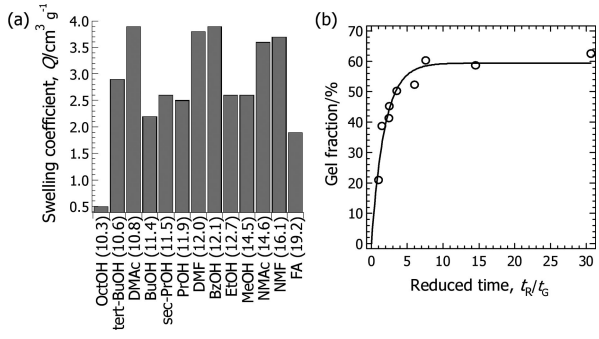

Figure 2. (a) Swelling coefficients for the gel sample D5-P0 with various solvents. The horizontal and vertical lines denote the name of solvents and their solubility parameters in cal$^{1/2}$ cm$^{-3/2}$, respectively. Solvents with solubility parameter ca. 12 cal$^{1/2}$ cm$^{-3/2}$ and amides except for FA are found to be the good solvents for GDMA network. (b) Time dependence of gel fraction with varying the reaction time for the sample D5-P0. Polymerization reaction is found to be finished within normalized time of 10.

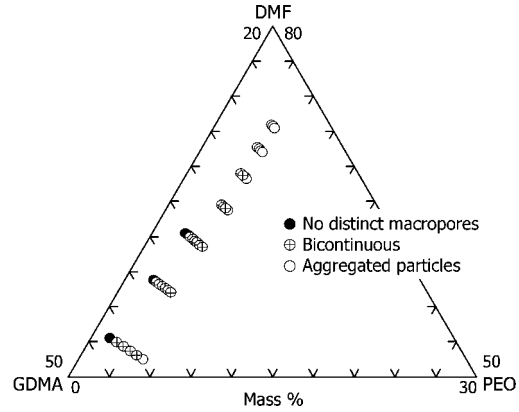

Figure 3. Triangular plot showing morphology−starting composition (in mass %) relationships. The grayed region in the full diagram is enlarged in the left partial diagram. Filled circle, circled cross, and open circle correspond to no distinct macropores, bicontinuous structure, and particle aggregates, respectively.

decreasing DMF while fixing GDMA/PEO both increase the phase separation tendency, as confirmed by the corresponding SEM pictures shown in Figure 4. Namely, from left to right in each row in Figure 4, it is confirmed that the bicontinuous morphology develops (i.e., pore size becomes larger) with increasing amount of PEO. By comparing D4-P0.25, D5-P0.25, and D6-P0.25 (from upper right to lower left), it can be confirmed that pore size becomes smaller with increasing amount of the solvent DMF. These tendencies are also consistent with the mercury intrusion data in Figure 5 and Table 2 as described later. With increasing tendency of phase separation, gel morphology changes from "no distinct macropores", "bicontinuous structure" to "aggregates of particles", as shown in Figure 3. Analogous to the silica sol−gel systems accompanied by phase separation,[4] this morphological change is attributed to the competitive occurrence of spinodal-type phase separation and structural freezing by gelation. The morphology with no distinct macropores obviously resulted from earlier gelation than the onset of phase separation. Bicontinuous structure is observed when phase separation and gelation almost concur with each other. When gelation takes place much later than the onset of phase separation, the originally bicontinuous gelling phase breaks up and becomes spherical to reduce the interfacial energy. The morphology with aggregates of particles therefore results accordingly. If gelation takes place further later than phase separation, precipitation of the gelling phase in the solvent will be observed, which is termed as "macroscopic double phase", but has not been observed in the present system. The fact that macroporous structure becomes finer with increasing amount of DMF with fixed GDMA/PEO ratio (D4-P0.25, D5-P0.25, and D6-P0.25) indicates that DMF acts as a good solvent that is consistent with the result of the swelling experiment. Namely, increasing amount of DMF retards the onset of phase separation in the system, resulting in smaller domains.

Figure 5 demonstrates the variations of macroporous properties of gels presented in Figure 4 characterized by mercury porosimetry. In each part (a) to (c) showing a fixed amount of DMF with varying PEO, both mean macropore size and total pore volume are increased with increasing amount of PEO. According to the previously reported DVB system,[15] only pore diameter varies and total pore volume is fixed when the amount of a polymeric agent PDMS is varied with a fixed amount of solvent. On the contrary, both the pore size and pore volume change with varying PEO in GDMA system. This is due to the large shrinkage in the present system. The DVB-derived network is highly rigid because of the presence of bulky aromatic rings and higher conversion. On the other hand, the network derived

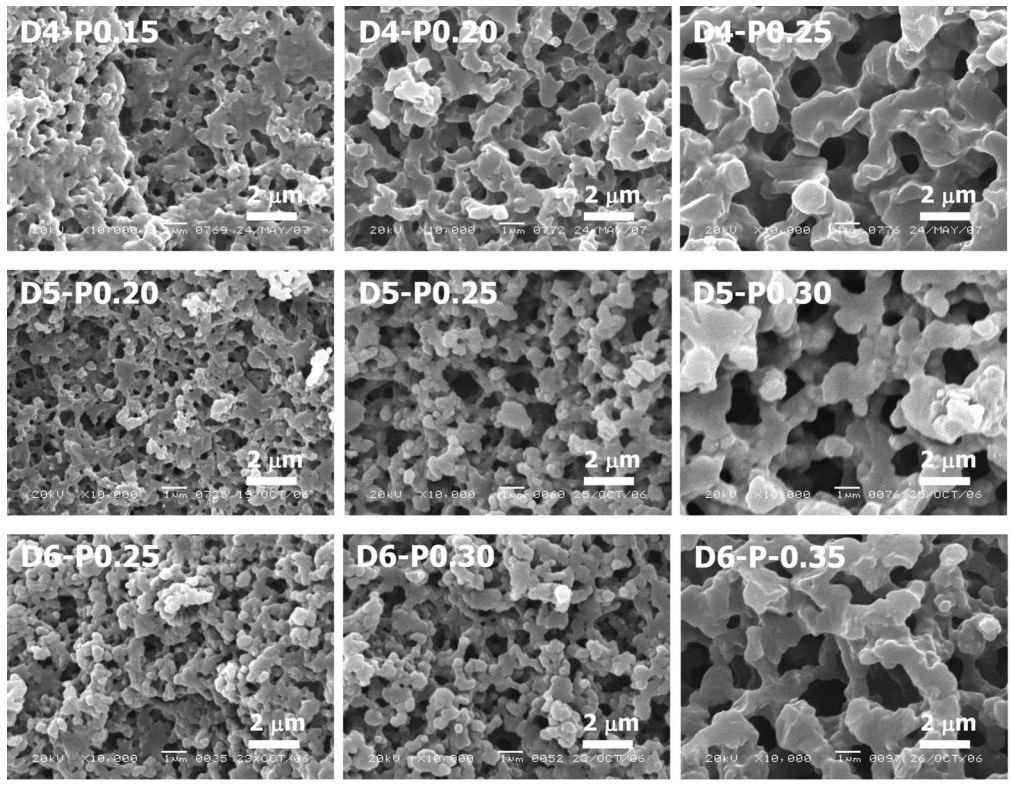

Figure 4. SEM photographs of the obtained macroporous samples (see Table 1 for the starting compositions and notations). Bicontinuous structure, which is typical resultant of spinodal decomposition, can be confirmed.

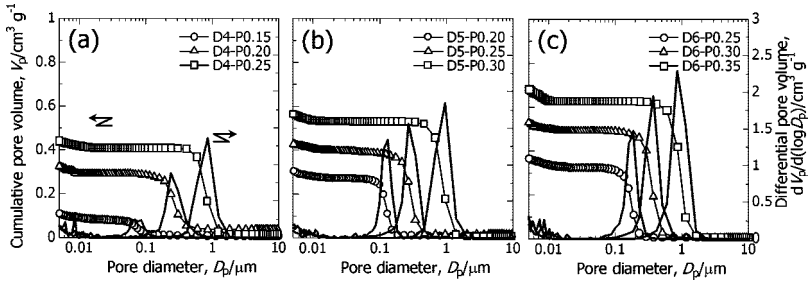

Figure 5. Pore size distributions obtained by mercury porosimetry. Each part shows the varying ratio of PEO/GDMA while DMF/GDMA is fixed. Increasing concentration of PEO makes pore size and volume larger, while increasing concentration of DMF makes pore size smaller.

Table 2. Pore Properties of Obtained Gels

	true density, d_s/g cm^{-3}	mean pore diameter, D_m/μm	total pore volume, V_t/cm^3 g^{-1}	porosity, ρ/%
D4-P0.15	1.31	0.0684	0.114	13.0
D4-P0.20	1.32	0.239	0.3267	30.0
D4-P0.25	1.32	0.845	0.441	36.8
D5-P0.20	1.31	0.130	0.310	28.8
D5-P0.25	1.33	0.269	0.431	36.4
D5-P0.30	1.33	0.967	0.567	42.9
D6-P0.25	1.33	0.187	0.367	32.7
D6-P0.30	1.33	0.374	0.529	41.3
D6-P0.35	1.34	0.855	0.687	47.8

from GDMA is weak due to the flexible network mainly consisting of carbon−carbon or carbon−oxygen single bonds and lower monomer conversion. The linear shrinkage of D5-P0.20, D5-P0.25, and D5-P0.30 was 35.8, 27.0, and 23.9%, respectively. This indicates that shrinkage becomes large for the gels with smaller pore sizes. This is consistent with the fact that the capillary pressure, which induces shrinkage, is inversely proportional to the pore size according to the Young−Laplace equation. With the fixed PEO/GDMA ratio, pore size becomes smaller with increasing DMF (see D4-P0.25, D5-P0.25, and D6-P0.25 in Figure 4) as described previously. In addition, the resultant total pore volume tends to increase with increasing amount of DMF because the solvent will be gradually excluded from gelling GDMA-rich phase into PEO-rich phase by syneresis. Here notice that the comparison should be made on the gels with similar pore diameters because shrinkage is substantially affected by the pore size. In other words, the reduction of pore volume by shrinkage increases with decreasing pore size. So when gels with similar pore diameters like D4-P0.25, D5-P0.30, and D6-P0.35 are compared, it can be confirmed that the pore volume increases with increasing DMF. The total pore volume is therefore determined mainly by the amount of solvent used and the extent of shrinkage. As for the porous properties inside the gel skeletons, no appreciable micro- and mesopores were found in these gels from nitrogen sorption measurements (not shown) because they were, if any, collapsed due to the large shrinkage during drying. Table 2 summarizes the pore properties obtained by mercury porosimetry and He pycnometry. Porosity can be controlled up to ∼48% in the present materials.

In Figure 6, the FTIR spectrum of PEO and those of the samples D5-P0 (washed) and D5-P0.30 (washed and unwashed) are presented. For PEO, the strong absorbance at 1095 cm^{-1} is characterized by the antisymmetric stretching mode of C−O−C entities. For the sample D5-P0 prepared without PEO, the strong

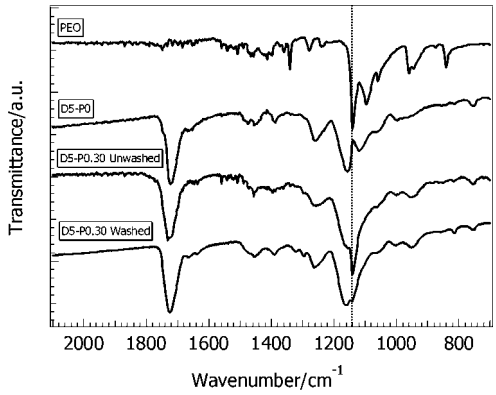

Figure 6. FTIR spectra of the samples and the additive PEO. By comparing characteristic absorption at 1095 cm^{-1} by ether groups of PEO and 1157 cm^{-1} by ester groups of methacrylate, it is found that a considerable amount of PEO is still incorporated in the methacrylate network even after the washing steps.

absorption bands located at 1157 and 1259 cm^{-1} stem from the methacrylate ester groups. The absorbance peak by ether groups of PEO, indicated by the vertical broken line, can also be found in the unwashed sample D5-P0.30, and even in the washed sample D5-P0.30, but naturally cannot be found in the sample D5-P0. When the unwashed and washed samples of D5-P0.30 are compared, it is noticed that the absorption by the ether groups of PEO is stronger in the unwashed sample. This in turn means that PEO that was separated from polymerizing GDMA-rich phase are removed by the simple washing step. However, a considerable amount of PEO is still trapped in the GDMA-derived networks even after the washing step as can be confirmed in the washed sample D5-P0.30. Absorptions by stretching modes of carbonyl groups C═O and C═C double bonds are found at 1724 and 1637 cm^{-1}, respectively. In washed D5-P0.30, it can be confirmed from the absorption at 1637 cm^{-1} that there are still some unreacted methacrylate groups in the gel networks. The pendant methacryl groups must be partially responsible for the low mechanical strength and large shrinkage during drying as described above. It was also revealed that glass transition temperature T_g of the sample D5-P0 is −22 °C from DSC measurements, and no glass transition was observed for the sample washed D5-P0.30. The low T_g may have resulted from the low cross-linking density, and no glass transition of the washed D5-P0.30 suggests that PEO incorporated in the network increases the rigidity.

TG-DTA curves for the washed sample of D5-P0 as well as washed and unwashed D5-P0.30 are displayed in Figure 7. According to the sample without PEO (D5-P0, part a), the loss of weight starts from around 260 °C by an endothermic thermooxidative degradation[21] and continues up to 550 °C without producing char. In the TG-DTA curves for the unwashed sample (D5-P0.30, part b), a small exothermic peak starting from around 200 °C is found, and it is attributed to PEO that was separated from the polymerizing GDMA-rich phase and was left on the GDMA-derived skeleton surface after drying. Main degradation starts from ca. 250 °C by an exothermic reaction, which is a little lower than that of the sample D5-P0 probably due to the thermal degradation of incorporated PEO molecules and the endothermic degradation peak observed in the sample D5-P0 has been masked. Degradation ends with a sharp exothermic peak starting from 380 °C, leaving very little char. Even for the washed sample prepared with PEO (D5-P0.30, part c), the degradation behavior is different from that prepared without PEO (D5-P0), probably due to inclusion of PEO deep inside the GDMA-derived gel networks which could not be removed by the washing steps. Degradation also starts from 250 °C and ends by the sharp exothermic peak from 400 °C, leaving very little char. Again, considering the results of FTIR and TG-DTA, PEO molecules that had been distributed in the phase other than GDMA-rich one (these PEO molecules remain on the surface of the GDMA-derived gel skeleton after drying) have been readily washed away by the easy washing step, but it cannot be neglected that a considerable portion of PEO still exists in the GDMA-derived networks even after washing. The rough estimation of the percentage of PEO molecules that were distributed in the phase other than GDMA-rich networks has been performed by TG-DTA at 200 °C where only such PEO molecules decompose. We found ca. 70% of PEO was distributed in the phase other than GDMA-rich one from the weight loss at 200 °C. Hence, phase separation is deduced to take place between GDMA-rich and PEO-rich phases. The mechanism is further discussed in the following section.

3.3. Origin and Mechanism of Phase Separation. The driving force of polymerization-induced phase separation can be discussed using the free energy change of mixing ΔG

$$\Delta G = \Delta H - T\Delta S \tag{1}$$

According to the Flory−Huggins mean field theory,[22] especially for a multicomponent polymeric system eq1 becomes

$$\Delta G \propto RT\left(\frac{\phi_1}{P_1}\ln\phi_1 + \frac{\phi_2}{P_2}\ln\phi_2 + \chi_{12}\phi_1\phi_2\right) \tag{2}$$

where ϕ_i ($0 < \phi_i < 1$) and P_i correspond to volume fraction and degree of polymerization of component i ($i = 1, 2$), respectively, and χ_{12} denotes interaction parameter between two components. For simplicity, the GDMA−PEO−DMF ternary system is reduced to the GDMA−PEO quasi-binary system here under the assumption that DMF simply acts as a cosolvent. We define component 1 and 2 as GDMA and PEO, respectively. The first and second terms on the right-hand side of eq2 show the contribution of conformational (translational) entropy and are denoted as the entropy terms, both of which always have negative values. Because the third term is related to the interaction energy between the two components, it is denoted as the enthalpy term. For the attractive interaction, χ_{12} is negative, which makes ΔG negative and promotes mixing. When the interaction is repulsive, on the contrary, χ_{12} become positive and may promote demixing depending on the magnitude of entropy terms. In this case, if the interaction is not too highly repulsive, the system prefers to be mixed in pursuit of gaining entropy. Since the increase of translational entropy upon mixing of polymers ($P_i \gg 1$) is not large for polymer systems, the system will be required to demix unless χ_{12} is small (or negative) enough to compensate the less negative contribution of the entropy terms. Negative χ_{12} is generally observed due to dipolar−dipolar interaction or hydrogen bonding, etc. With the progress of polymerization of at least one component, ΔG in a system increases, and phase separation is induced upon the sign of ΔG turns positive. This is called polymerization-induced phase separation and is the main cause of the phase separation observed in the present system.

As shown in the previous section, the driving force of phase separation is deduced to be the entropic loss of free energy upon polymerization of GDMA, and one separated phase mainly consists of the GDMA-derived networks and the other mainly PEO. The values of solubility parameter for GDMA gel and PEO are ca. 12 $cal^{1/2}\ cm^{-3/2}$ (from the swelling experiment described above) and ∼9.5 $cal^{1/2}\ cm^{-3/2}$ (for $M_w = 20\,000$),[23] respectively. Since χ_{12} is proportional to the square of the difference of solubility parameters, χ_{12} can be treated as positive enough. The solvent DMF acts as a cosolvent and is considered to be distributed in both phases. In such a situation, the increase of P_1 increases ΔG in the course of polymerization while P_2 and the other parameters remain constant. Note that χ_{12} may be

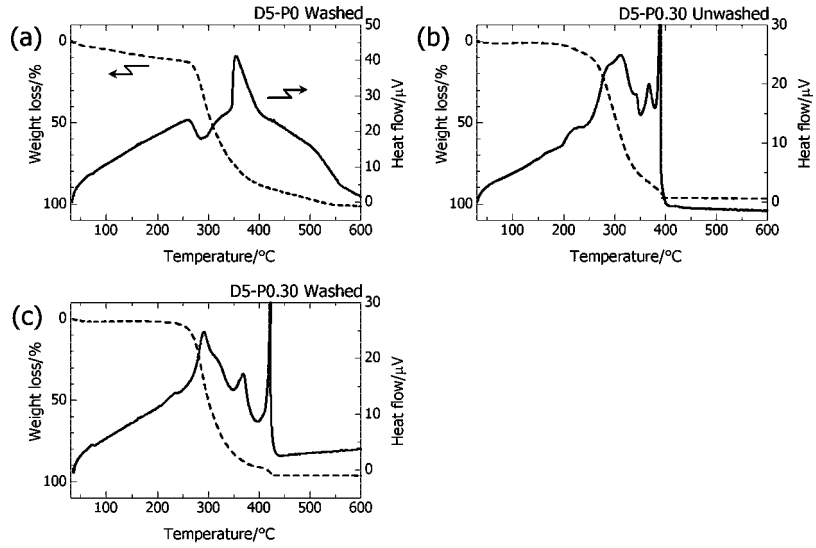

Figure 7. Curves of thermogravimetry (TG, broken lines) and differential thermal analysis (DTA, solid lines) of the samples (a) washed D5-P0, (b) unwashed D5-P0.30, and (c) washed D5-P0.30.

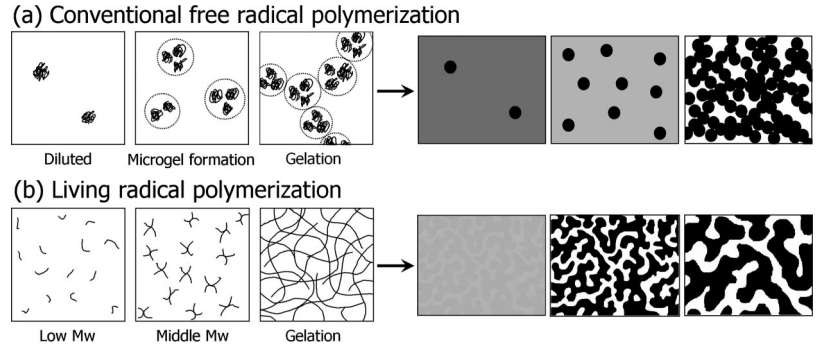

Figure 8. Comparative illustrations of (a, left) conventional free radical polymerization in a solvent leading to heterogeneous cross-linking and (b, left) living radical polymerization leading to homogeneous cross-linking. The heterogeneous polymerization gives concentration fluctuation in the gel network, and in an extreme case, the microgels formation occurs in the solvent which suffocates the isotropic spinodal decomposition (a, right). Conversely, in the case of living radical polymerization (b, right), isotropic spinodal decomposition will be induced under the existence of another polymeric agent. In this case, homogeneous (nonporous) gels will be resulted if no polymeric agent is added. Note that the left parts showing gelation are in the molecular scale, and the right parts showing phase separation are in micrometers scale. After refs 39 and 40.

changed as well, but it can be neglected because polar groups such as ester and hydroxyl groups, which might cause the change in χ_{12}, remain unreacted. Thus, the phase separation is generated when ΔG becomes positive due to the loss of entropy by the polymerization of GDMA.

The other probable situation arises when PEO has an attractive interaction with GDMA. In this case, PEO should be strongly hydrogen-bonded with GDMA-derived species ($\chi_{12} < 0$), and these two make a kind of complex. The system would phase-separate into the GDMA−PEO complex and DMF. Obviously, this is not the case in the present case as have been described so far. The former mechanism is a more general for multicomponent polymer systems as can be found in a lot of polymer blend systems.[24−26] The latter one is specific to a strong hydrogen-bonding system of polymer blends[27] and of inorganic systems such as PEO and acidic metal oxides.[28−30]

3.4. Phase Separation in Heterogeneous vs Homogeneous Networks. The theory of gel formation is established by Flory and Stockmayer and called the FS theory.[31−35] The FS theory provides an ideal random gel formation mechanism where no intramolecular cyclization is considered, and the gelation is defined as the point at weight-average molecular weight diverges. In real systems, however, the gelation reaction is composed of two competitive reactions: intermolecular and intramolecular cross-linking. Large heterogeneity, i.e., spatially inhomogeneous distribution of cross-linking points resulted from a wide distribution of molecular weight, is usually found. This is obviously due to the abrupt nature of free radical systems, and such heterogeneous cross-linking apparently makes the network deviate from the FS theory. In an extreme case, such locally coherent domains may be segregated from solvent to generate microgels as a result of the conventional free radical polymerization reactions.[36−38] Free radical polymerization generates (dead) polymers with high degree of polymerization even in the very early stage of the reaction, which results in microgels formation even in a good solvent in some cases. Microgels react with other microgels more efficiently than with monomers. Eventually they segregate from the solvent especially when the monomer concentration is so low that intramolecular cyclization is more likely to occur. The gel formation in this case is therefore regarded as the weak linkages of microgels. After drying the solvent, macroporous morphology consisting of submicron or micron-sized microgel particles results in this way as shown in Figure 8a. In the case where such strong segregation would not occur, infinite network forms with the heterogeneous cross-linking. The heterogeneous cross-linking generates the concentration fluctuation throughout the network that will compete with spinodal decomposition as discussed later.

Meanwhile, Ide and co-workers demonstrated that the living radical polymerization by a nitroxide-mediated system leads to

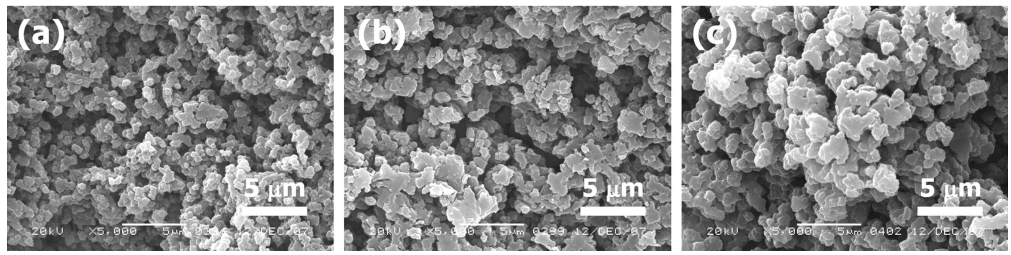

Figure 9. GDMA gels that are not prepared by ATRP but by the conventional free radical polymerization using 1 mol % AIBN as initiator and reacted at 60 °C, 24 h. The other compositions, GDMA, DMF, and PEO, are the identical to (a) D5-P0.20, (b) D5-0.25, and (c) D5-0.30, respectively. The obtained macroporous morphologies are obviously different from that obtained by ATRP.

the formation of a highly homogeneous cross-linking, and the number of cross-links at the gel point was enough close to the FS theory whereas that for the conventional free radical system is much larger.[39,40] Various measurements such as gel fraction, swelling ratio, and average molecular weight as a function of monomer conversion have proven the formation of homogeneous cross-linking. Jiang et al. also confirmed the similar gelation behavior using cross-linking methacrylates via ATRP.[41,42] In these cases, the fact that gelation occurred at higher conversions than that of the FS theory predicts suggests the cyclization and existence of pendant vinyl groups. In the case of GDMA gels presented here, also confirmed are the existence of pendant vinyl groups by FTIR, and mechanically weak characters leading to large shrinkage may have been resulted from the formation of loops and/or incomplete cross-links. As pointed out by Aoki et al., intermolecular or intramolecular reactions of GDMA is strongly directed by hydrogen bonding of in-between hydroxyl groups on GDMA molecules;[43] it therefore can be assumed that either inhibited cross-linking or preferred cyclization is responsible for the mechanical weakness. Nevertheless, highly homogeneous distribution of cross-linking points allowed the homogeneous gel formation in a good solvent as illustrated in Figure 8b (left). As shown in the right part of Figure 8b, spinodal decomposition will be induced with the addition of a proper polymeric agent. Free radical polymerization, on the other hand, shows a stronger tendency to form heterogeneous cross-linking, and in some cases microgels segregate prior to the onset of spinodal decomposition even in a good solvent and without a polymeric agent as shown in the right part of Figure 8a. Moreover, this heterogeneity in submicron or microns scales prohibits the formation of isotropic compositional fluctuation with competitive wavelength, which is typically submicrons,[24] directed in the early stage of spinodal decomposition. Especially for gelling systems, such heterogeneous network cannot be reorganized in a diffusive manner to allow isotropic spinodal decomposition due to the significantly low mobility which resulted from cross-linking, and spinodal decomposition therefore cannot develop in a large scale. In other words, since the heterogeneous cross-linking and isotropic spinodal decomposition (and also infinite network formation) are the competitive processes, the dimension of heterogeneity of cross-linking mainly determines the final morphology. In the case of weak segregation, since spinodal decomposition is to be induced in a relatively highly cross-linked heterogeneous network, it cannot develop well in the network. Hence, if gelation takes place soon after the onset of phase separation and the heterogeneity is not very high, bicontinuous morphology with very short wavelength (typically a few hundred nanometers) generated in the initial stage of spinodal decomposition will be frozen by gelation. We have indeed observed this kind of very fine porous morphology in many conventional radical polymerization systems, but it cannot develop in a larger scale. When spinodal decomposition occurs well before heterogeneous cross-linking due to the strong immiscibility, the bicontinuous morphology formed by spinodal decomposition would be completely disturbed by the following heterogeneous cross-linking that occurs inside one of the separated phases. Therefore, avoiding heterogeneous cross-linking is the most critical issue to overcome in order to obtain macroporosity by isotropic spinodal decomposition. The extent of heterogeneity that is allowed to induce isotropic spinodal decomposition must be determined using a scattering technique in the near future.

In order to confirm this idea, dried gels prepared with the conventional free radical polymerization using AIBN as initiator have been prepared and are given in Figure 9. The other compositions such as GDMA, PEO, and DMF are identical to D5-P0.20, D5-P0.25, and D5-P0.30. These dried gels show heterogeneous porous morphologies resulting from the disturbance of isotropic spinodal decomposition by the heterogeneous cross-linking. In this free radical system, even when no PEO is added, somewhat turbid gel has been obtained whereas the equivalent sample D5-P0 prepared by ATRP is transparent. These facts support the above-mentioned idea on heterogeneous cross-linking vs isotropic spinodal decomposition.

Consequently, combined with the facts reported in the previous paper,[15] it can be summarized that living polymerization systems that afford a fine control of polymerization dynamics can be applied to produce well-defined bicontinuous macroporous morphology formed through spinodal decomposition that induced during the transition from solution to gel. Since the formability by the homogeneous cross-linking may further applied to the addition of smaller pores (micro- or mesopores on the nanometer scale) inside the gel skeletons, hierarchically pore structures simultaneously having macropores for fast fluid transport and micro- or mesopores for increasing surface areas, would be expected, and it is currently underway.

4. Conclusion

Macroporous cross-linked polymer monoliths with well-defined bicontinuous macroporous morphology are prepared via atom transfer radical polymerization (ATRP) of 1,3-glycerol dimethacrylate (GDMA) under the existence of a polymeric agent, poly(ethylene oxide) (PEO) in a solvent *N*,*N*-dimethylformamide (DMF). The addition of the polymeric agent induces thermodynamic instability during polymerization of GDMA, resulting in spinodal decomposition to give well-defined macropores with cocontinuous skeletons. Obtained dried gels show bicontinuous macroporous morphology and micro- and mesopore volumes are found to be considerably small. Macropore size and volume can be easily controlled in a way that varying the concentrations of PEO and/or DMF, and it is found that pore size and pore volume are affected by the large shrinkage during drying.

Although it is found that a certain portion of PEO is distributed in the GDMA-rich phase, the phase separation is deduced to occur between GDMA-rich and PEO-rich phases. Living polymerization like ATRP, as well as the nitroxide-mediated polymerization system, affords the formation of homogeneous networks, and spinodal decomposition can be

induced to form well-defined macroporous morphology in such a homogeneous matrix. This is contrastive to the conventional free radical polymerization that normally results in significant heterogeneity and, in an extreme case, results in segregation of microgels. The present facile synthesis of well-defined macroporous polymer monoliths using highly versatile ATRP will provide us more extended selection of monomers and open the way to a prevailed use of various functional porous polymer monoliths as separation media, catalyst supports, and membranes, etc.

Acknowledgment. We thank Prof. Ken Hosoya at Tohoku University for introducing us to the ATRP procedure. Tomoo Hasegawa is also gratefully acknowledged for his experimental contribution. The present work was partly supported by a Grant for Practical Application of University R&D Results under the Matching Fund Method from New Energy and Industrial Technology Development Organization (NEDO), Japan. This research was also partly supported by the Global COE Program "International Center for Integrated Research and Advanced Education in Materials Science" (No. B-09) of the Ministry of Education, Culture, Sports, Science and Technology (MEXT) of Japan, administrated by the Japan Society for the Promotion of Science (JSPS). Also, this study was supported by the Grant-in-Aid for Young Scientists (B) (No. 20750177) from the MEXT, Japan.

References and Notes

(1) Tanaka, N.; Kobayashi, H.; Ishizuka, N.; Minakuchi, H.; Nakanishi, K.; Hosoya, K.; Ikegami, T. *J. Chromatogr. A* **2002**, *965*, 35–49.
(2) Vervoort, N.; Gzil, P.; Baron, G. V.; Desmet, G. *Anal. Chem.* **2003**, *75*, 843–850.
(3) Saito, H.; Nakanishi, K.; Hirao, K.; Jinnai, H. *J. Chromatogr. A* **2006**, *1119*, 95–104.
(4) Nakanishi, K. *J. Porous Mater.* **1997**, *4*, 67–112.
(5) Kanamori, K.; Yonezawa, H.; Nakanishi, K.; Hirao, K.; Jinnai, H. *J. Sep. Sci.* **2004**, *27*, 874–886.
(6) Gusev, I.; Huang, X.; Horváth, C. *J. Chromatogr. A* **1999**, *855*, 273–290.
(7) Svec, F. *J. Sep. Sci.* **2004**, *27*, 747–766.
(8) Macintyre, F. S.; Sherrington, D. C. *Macromolecules* **2004**, *37*, 7628–7636.
(9) Rohman, G.; Grande, D.; Lauprêtre; Boileau, S.; Guérin, P. *Macromolecules* **2005**, *38*, 7274–7285.
(10) Tsujioka, N.; Hira, N.; Aoki, S.; Tanaka, N.; Hosoya, K. *Macromolecules* **2005**, *38*, 9901–9903.
(11) Peters, E. C.; Svec, F.; Fréchet, J. M. J.; Viklund, C.; Irgum, K. *Macromolecules* **1999**, *32*, 6377–6379.
(12) Viklund, C.; Nordström, A.; Irgum, K.; Svec, F.; Fréchet, J. M. J. *Macromolecules* **2001**, *34*, 4361–4369.
(13) Sinner, F. M.; Buchmeiser, M. R. *Angew. Chem., Int. Ed.* **2000**, *39*, 1433–1436.
(14) Sinner, F. M.; Buchmeiser, M. R. *Macromolecules* **2000**, *33*, 5777–5786.
(15) Kanamori, K.; Nakanishi, K.; Teiichi, H. *Adv. Mater.* **2006**, *18*, 2407–2411.
(16) Wang, J.-S.; Matyjaszewski, K. *J. Am. Chem. Soc.* **1995**, *117*, 5614–5615.
(17) Xia, J.; Matyjaszewski, K. *Macromolecules* **1997**, *30*, 7697–7700.
(18) Roice, M.; Subhashchandran, K. P.; Gean, A. V.; Franklin, J.; Rajasekharan Pillai, V. N. *Polymer* **2003**, *44*, 911–922.
(19) Roice, M.; Rajasekharan Pillai, V. N. *J. Polym. Sci., Part A: Polym. Chem.* **2005**, *43*, 4382–4392.
(20) Aoki, H.; Kubo, T.; Ikegami, t.; Tanaka, N.; Hosoya, K.; Tokuda, D.; Ishizuka, N. *J. Chromatogr. A* **2006**, *1119*, 66–79.
(21) Wojcik, A. B. *J. Polym. Sci., Part A: Polym. Chem.* **1990**, *39*, 179–187.
(22) Flory, P. J. *Principles of Polymer Chemistry*; Cornell University Press: Ithaca, NY, 1971.
(23) Martuscelli, E.; Silvestre, C.; Addonizio, M. L.; Amelino, L. *Makromol. Chem.* **1986**, *187*, 1557–1571.
(24) Izumitani, T.; Hashimoto, T. *J. Chem. Phys.* **1985**, *83*, 3694–3701.
(25) Hashimoto, T.; Itakura, M.; Hasegawa, H. *J. Chem. Phys.* **1986**, *85*, 6118–6128.
(26) Jinnai, H.; Nishikawa, Y.; Morimoto, H.; Koga, T.; Hashimoto, T. *Langmuir* **2000**, *16*, 4380–4393.
(27) Moskala, E. J.; Howe, S. E.; Painter, P. C.; Coleman, M. M. *Macromolecules* **1984**, *17*, 1671–1678.
(28) Nakanishi, K.; Komura, H.; Takahashi, R.; Soga, N. *Bull. Chem. Soc. Jpn.* **1994**, *67*, 1327–1335.
(29) Nakanishi, K.; Soga, N. *Bull. Chem. Soc. Jpn.* **1997**, *70*, 587–592.
(30) Mathur, S.; Moudgil, B. M. *J. Colloid Interface Sci.* **1997**, *196*, 92–98.
(31) Flory, P. J. *J. Am. Chem. Soc.* **1941**, *63*, 3083–3090.
(32) Flory, P. J. *J. Am. Chem. Soc.* **1941**, *63*, 3091–3096.
(33) Flory, P. J. *J. Am. Chem. Soc.* **1941**, *63*, 3096–3100.
(34) Stockmayer, W. H. *J. Chem. Phys.* **1943**, *11*, 45–55.
(35) Stockmayer, W. H. *J. Chem. Phys.* **1944**, *12*, 125–131.
(36) Chiu, Y. Y.; Lee, L. J. *J. Polym. Sci., Part A: Polym. Chem.* **1995**, *33*, 257–267.
(37) Chiu, Y. Y.; Lee, L. J. *J. Polym. Sci., Part A: Polym. Chem.* **1995**, *33*, 269–283.
(38) Okay, O. *Polymer* **1999**, *40*, 4117–4129.
(39) Ide, N.; Fukuda, T. *Macromolecules* **1997**, *30*, 4268–4271.
(40) Ide, N.; Fukuda, T. *Macromolecules* **1999**, *32*, 95–99.
(41) Jiang, C.; Shen, Y.; Zhu, S.; Hunkeler, D. *J. Polym. Sci., Part A: Polym. Chem.* **2001**, *39*, 3780–3788.
(42) Yu, Q.; Zhou, M.; Ding, Y.; Jiang, B.; Zhu, S. *Polymer* **2007**, *48*, 7058–7064.
(43) Aoki, H.; Hosoya, K.; Norisuye, T.; Tanaka, N.; Tokuda, D.; Ishizuka, N.; Nakanishi, K. *J. Polym. Sci., Part A* **2006**, *44*, 949–958.

MA800563P